Fuzzy PI Model Predictive DTC for Gas Pressure Regulated Power Generation System

Dong Wei [*1], Ruo-Chen Zhao [*2], Ya-Xuan Xiong[*3] Ming-Xin Zuo[*4] and Hao-Qing Zhang[*5]

[*1] Department of electrical and Information Engineering, Beijing University of Civil Engineering and Architecture & Beijing Key Laboratory of Intelligent Processing for Building Big Data, ,Beijing
E-mail: weidong@bucea.edu.cn
[*2] Same as fist author
E-mail: zhaoruochen001@163.com
[*3]S School of Environmental and Energy Engineering , Beijing University of Civil Engineering and Architecture, Beijing
E-mail: xiongyaxuan@bucea.edu.cn.
[*4] Same as fist author
E-mail: mingxinzuo@163.com
[*5] China Resources Land(Beijing) Co，ltd , Beijing
E-mail: 1270501169@qq.com

Abstract. In the gas supply system, the pressure regulation system is required to regulate the gas from high pressure to low pressure on the customer side, where the pressure energy can be recovered by the expander driven generator operation. However, the existing regulator system and generator torque control loop have the problem of difficult PI parameter adjustment, in addition to the strong non-linearity of the hysteresis comparator and switching table in the traditional direct torque control, which causes difficulties in controller design and leads to large fluctuations in generator torque. To this end, this paper constructs fuzzy PI controllers for expander pressure regulation and generator torque control loops respectively, and realizes adaptive adjustment of PI parameters; meanwhile, with the control objective of making the generator torque and flux linkage stable, the optimal voltage vector calculation is performed directly by using model predictive controller instead of the hysteresis comparator and vector switching table in the generator internal loop control loop, which improves the efficiency of the algorithm and improves the control performance by delay compensation. The simulation experimental results show that the proposed control algorithm reduces the generator torque fluctuation range by 84.5%, the speed fluctuation range by 66.7%, and the three-phase current fluctuation range by 65.6% compared with the traditional direct torque control algorithm.

Keywords: Fuzzy PI Control, Model Predictive Control, DTC, Power Generation System

1. INTRODUCTION

In the gas supply system, the pressure regulating system needs to regulate the gas pressure from 6MPa or more at the gas source to about 3×10-3MPa for residential customers, which requires multiple stages of pressure regulation, and this process contains a large pressure energy change using the expander with the generator to recover this pressure energy, forming a gas regulator power generation system, can improve energy utilization. In the process of gas supply, the expander drives the coaxially connected Permanent Magnet Synchronous Generator (PMSG) to rotate and generate electricity, while the high-pressure gas is expanded and depressurized and then stabilized for downstream users to achieve pressure energy recovery [1]. However, when the gas consumption of downstream users changes, it will lead to changes in the outlet pressure of the expander causing changes in the output torque of the expander, thus making the PMSG speed connected to the straight shaft of the expander unstable, and because the system has multiple loops, the control is more complex, and there is no relevant research results for gas pressure energy recovery, resulting in a large amount of wasted energy.

In order to improve the stability of the generator speed, it is first necessary to make the expander outlet pressure stable, and the commonly used method is to install an electric regulator at the outlet of the expander, and the expander outlet pressure is calculated from the user-side gas consumption and used as a given value for the PID controller in the regulator system, and the PID controller gives the control signal of the electric mechanism according to the deviation between the given value and the actual expander outlet pressure, thus regulating the outlet pressure of the regulator [2]. However, due to the uncertainty of the customer-side pressure of the gas system, when the customer-side pressure changes, resulting in changes in the outlet pressure of the expander and thus its output torque, the originally adjusted PID parameters may not be suitable for the current operating conditions, which may not only degrade the control performance, but also cause the generator to block or fly when the generator torque cannot quickly follow the expander output torque [3].

Therefore, when the output torque of the expander changes, the PMSG needs to be controlled so that the PMSG can quickly follow the output torque of the expander. Currently, the existing results in PMSG control usually use the Direct Torque Control (DTC) control method. The DTC algorithm places emphasis on direct control of the electromagnetic torque of the PMSG without complex mathematical transformations, and is therefore widely used for generator control. The outer loop of the direct torque control is the speed loop, which usually uses PI control to make the generator speed follow the speed of the expander in real time; the inner loop uses a hysteresis comparator to input the flux linkage, torque and their set values into the comparator and then obtain the deviation, and then use this deviation with the voltage switching vector table to select the appropriate voltage vector to control the amplitude of the flux linkage and torque to eliminate the deviation of the magnetic chain and torque [4]. However, when the threshold value of the hysteresis comparator is changed, the output of the hysteresis comparator will change and the voltage vector obtained from the table may not be able to stabilize the magnitude of the flux linkage and torque. In addition, the delay caused by the signal transmission will cause the voltage vector of the query to be unsuitable for the current moment, which will lead to large fluctuations in torque.

To solve the above problems, several scholars have conducted related researches in recent years. Zhu Renshuai [5] et al. used an improved Active Disturbance Rejection Controller(ADRC) to replace the PI controller to control the motor in order to solve the problem that the PI controller cannot meet the high performance control under the action of internal parameters and external disturbances. The results improve the dynamic characteristics and robustness of the control system by establishing a tracking differentiator, an extended state observer, and a nonlinear state error feedback control law. To improve the generator control accuracy and control system adaptive capability. Chen Guangwei et al [6] studied a space vector pulse width modulation (SVPWM)-based direct torque control algorithm for generators to reduce the error between the actual and given values of torque by calculating the sector in which the flux linkage is located during a switching cycle, while determining the time of action of each voltage vector and the moment of switching on, and synthesizing an optimal voltage vector to reduce the error between the actual and given values of torque, thus reducing the motor torque fluctuation. Wang Y et al [7] used a torque-angle sinusoidal linear control method by calculating the dual integral values between the torque angle, motor speed and the DC voltage at both ends of the converter, and obtaining the optimal switching quantity and its action time according to the switching table, thus enabling the speed and torque to converge simultaneously with only one adjustment. Ghamri A et al [8] used an artificial neural network approach to construct an artificial neural network model with torque, flux linkage error and the sector where the flux linkage is located as inputs and switching quantities as outputs, and used the model to replace the nonlinear hysteresis comparator and switching table in conventional direct torque control to reduce the torque fluctuation of the motor and improve the system dynamic performance. Thamizhazhagan P [9] et al. used the Adaptive Vector Reference Control (AVRC) method to drive a three-phase converter and established a centralized control system in the AVRC structure to track torque and reduce energy losses by improving the switching conditions of the converter.

The above research results mostly focus on the motor running in the electric state without the disturbance brought by the prime mover, while the gas-regulated power generation system studied in this paper is susceptible to the time-varying influence of the gas consumption of downstream users, and the system is characterized by variable disturbance amplitude and high disturbance frequency. The PI controller in the above research results lacks parameter adaptive tuning capability and cannot adapt well to the variable operating conditions in gas pressure regulator power generation systems; the ADRC can improve the system performance compared with the PI control, but its structure is complex and requires more parameters to be adjusted artificially, and the parameters also lack adaptive capability. In addition, to address the problem of generator torque and flux linkage fluctuations due to the strong nonlinearity of the hysteresis comparator and switching table in the conventional DTC, the existing method of building artificial neural networks requires the collection of relevant data under all dynamic operating conditions of the generator for training, which is a large training sample and difficult to collect data.

In this paper, a direct torque control algorithm based on fuzzy PI and model prediction for gaspressure regulator power generation system is proposed to address the above problems, in which the fuzzy PI controller takes the error between the expander outlet pressure, the generator speed and the set value and the rate of change of the error as inputs to control the generator torque. In addition, due to the strong nonlinearity of the hysteresis comparator and switching table in the inner loop of direct torque control, the generator torque and flux linkage fluctuate greatly. Therefore, this paper uses Model Precitive Control (MPC) instead of the existing hysteresis comparator and switching table to directly calculate the optimal voltage vector with the control objective of stabilizing the generator torque and flux linkage, to achieve delay compensation on the one hand, and to improve the efficiency of the algorithm by avoiding table checking on the other hand, so as to improve the system performance.

2. COMPOSITION AND PRINCIPLE OF GAS PRESSURE REGULATING POWER GENERATION SYSTEM

The structure diagram of the gas pressure regulator power generation system is shown in Figure 1, which consists of a regulator system, an expander, and a PMSG machine side/grid side converter.

The structure diagram of the gas pressure regulator power generation system is shown in Figure 1, which consists of a regulator system, an expander, and a PMSG machine side/grid side converter. In Figure 1, the pressure regulator system calculates the gas pressure downstream of the gas transportation pipeline based on the gas consumption of downstream customers, and adjusts it with the regulator inside the regulator system to stabilize the downstream gas pressure; the expander is used to recover the pressure energy in the gas transportation pipeline and provide torque to the PMSG through the main shaft. Expansion machines are divided into volumetric and velocity types depending on the energy conversion method. The volumetric type, represented by the single screw expander, is widely used because of its low flow rate and high expansion ratio. The single-screw expander is driven by the high-pressure gas into the working chamber to rotate the internal star wheel

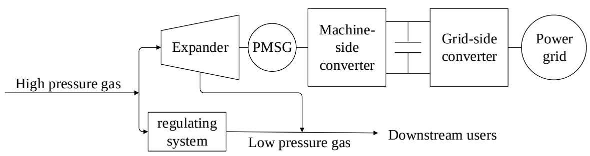

Fig.1 Structure diagram of gas pressure regulation and power generation system

and the screw, and the pressure energy is converted into mechanical energy through the spindle output torque to realize the expansion work [10] The torque of the PMSG follows the output torque of the expander to achieve rotating power generation. The machine side converter in Figure 1 is used to control the torque of the generator; the capacitor connected in parallel between the machine side/grid side rectifier on the busbar is used for voltage regulation; the grid side converter converts the DC power on the busbar to AC power and sends it to the grid according to the demand on the grid side.

The high pressure gas enters the expander to expand and do work, which drives the generator to rotate and generate electricity, and the generator speed is controlled by the machine side converter to stabilize, and the electricity generated by the PWM converter is inverted and can be delivered to the grid if it meets the grid requirements. However, changes in gas consumption by downstream customers can cause sudden pressure changes at the expander outlet, resulting in changes in the expander output torque, which in turn can cause instability in the speed of the coaxially connected generator. Therefore, it is necessary to study the generator control algorithm to control the torque of the generator using the machine side converter when the gas consumption of downstream users changes, so that it can quickly track the change of the output torque of the expander to achieve torque balance and keep the generator speed stable.

3. MATHEMATICAL MODEL OF SYSTEM

In order to implement the PMSG model predictive direct torque control algorithm, the mathematical model of the power generation system needs to be established. Also, for the purpose of conducting simulation experiments, this paper establishes the corresponding mathematical models for the regulator, expander and PMSG in the gas pressure regulator power generation system, respectively.

3.1. Mathematical model of pressure regulator

The pressure regulator is located in the pressure regulating system in Figure 1, and from its location in the figure, it is clear that the outlet pressure of the regulator is the pressure of the low pressure gas on the downstream side of the gas transportation pipeline. To maintain a stable outlet pressure, the motor in the electric regulator needs to be controlled. Gas electric pressure regulator consists of three parts, respectively, electric regulating valve, controller and collection unit. Data acquisition unit will be collected by the valve outlet pressure signal after processing and transmitted to the controller, the controller is processed through the pressure regulator algorithm output control signal, drive the motor through the transmission device to drive the valve stem to change the valve opening, so that the valve outlet pressure is maintained within the safe range.

The physical meaning of each symbol in the motor actuator in the regulator is given in Table 1

Where the relationship between the stem displacement H and and the mechanical angle θ1 i of the motor drive is expressed by the transfer function as equation (1) [11]:

Tab.1 The physical meaning of each symbol of the pressure regulator motor actuator

Symbol	Physical meaning
ω_n	Natural angular frequency
B	Viscous damping coefficient of motor shaft
K	Motor torsion angle
ζ	Screw efficiency
K_i	Sensor feedback gain
i	Transmission ratio of reduction mechanism
J	Moment of inertia of motor shaft
J_1	Equivalent moment of inertia on the motor shaft
J_2	Equivalent moment of inertia on the screw
B_2	Screw shaft viscous damping coefficient
L	Stem lead

$$H(s)=\frac{Y_1\theta_1-Y_2(s^2+X_1s+X_2)}{Z_3s^3+Z_2s^2+Z_1s+Z_0} \tag{1}$$

Where:

$$X_1=(B/J)$$
$$X_2=\omega_n^2$$
$$Y_1=L\omega_n^2/2\pi$$
$$Y_2=L^2F_L/4K\pi^2\zeta\mathrm{i}$$
$$Z_3=(iB+B_2/i)/K$$
$$Z_2=(B/J)(iB+B_2/i)+i$$
$$Z_1=\omega_n^2(iB+B_2/i)+(B/j)$$
$$Z_0=i\omega_n^2$$

Since the difference between the calculated results of Y_2 and Z_3 differ very little [12], the mathematical model of the motor actuator in the electric regulator is approximated by the second-order system, so (1) can be rewritten as:

$$H(s)=\frac{Y_1\theta_1}{Z_2s^2+Z_1s+Z_0} \tag{2}$$

Also because the relative valve opening x is related to the valve displacement H as follows:

$$X=H/L \tag{3}$$

Thus (2) can be rewritten as (4):

$$H(s)=\frac{Y_1/L\theta_1}{Z_2/Ls^2+Z_1/Ls+Z_0/L} \tag{4}$$

The relationship between the valve opening x and the flow rate Q is shown in (5):

$$Q=ax+b \tag{5}$$

Where *a* is the flow coefficient and is a constant and *b* is a constant.

Since the outlet pressure, flow rate and gas temperature of the valve are constant values, the flow rate of the gas is basically linear with its pressure at this time. Therefore, the relationship between pressure and flow rate can be approximated by (6):

$$P_2=kQ+c \tag{6}$$

Where c is the uncertainty time variable and k is the uncertainty time variable.

Combined with the relationship between the motor rotation mechanical angle of the motor actuator of (4) and the relative opening of the valve, the mathematical model of the input electro-mechanical angle of the gas electric regulator system and the output valve outlet pressure can be derived. Its state space equation is shown in (7):

$$\begin{cases} x_1 = x_2 \\ \dot{x}_2 = f(x,t) + g(x,t)u + d(t) \\ y = x_1 \end{cases} \tag{7}$$

Where $x = [x_1 , x_2]$is the state vector, x_1 denotes the valve outlet pressure, and x_2 denotes the rate of change of the valve outlet pressure.

The expressions of each function in (7) are:

$$f(x,t) = -\frac{Z_1}{Z_2}x_2 - \frac{Z_0}{Z_2}x_1 \tag{8}$$

$$g(x,t) = \frac{kY_1}{Z_2} \tag{9}$$

$$d(t) = P_1\frac{Z_0}{Z_1} + d_1(t) \tag{10}$$

Where $d_1(t)$ denotes all external disturbances such as friction on the valve stem, the magnitude of parameter deviation from the ideal value, etc.

In this paper, the values of each physical parameter of the system are selected according to the literature [13], so the mathematical model of the gas electric regulator is shown in (11):

$$\begin{cases} x_1 = x_2 \\ \dot{x}_2 = -10.31x_2 - 12.89x_1 + 65u + d(t) \\ y = x_1 \end{cases} \tag{11}$$

3.2. Mathematical Model of Expander

During the operation of the expander, assuming that it has good internal adiabaticity, its operating process can be regarded as an adiabatic expansion process, when the energy transfer relationship of the expander is shown in (12) [14]:

$$E_1 + J_1 = E_2 + J_2 + W + Q \tag{12}$$

E_1 , E_2 are the energy of the mass entering and leaving the expander, J_1,J_2 are the work done by them to push the expander, W is the output shaft work of the expander, and Q is the heat exchanged between the expander and the outside world.

Based on the defining equation of enthalpy, (12) can be rewritten as (13):

$$W = \Delta E + \Delta J \tag{13}$$

Where ΔE is the difference in energy flowing into and out of the expander, and ΔJ is the difference in work flowing out due to the inflow of the expander.

Based on the defining equation of enthalpy, (13) can be rewritten as (14):

$$W = C_p(T_{\text{in}} - T_{on}) \tag{14}$$

$$T_{on} = T_{in}\left(\frac{P_2}{P_1}\right)^{\frac{k-1}{k}} \tag{15}$$

The output torque model of the expander can be deduced as:

$$T_m = \frac{W}{n} = mC_pT_{in}\left(1 - \frac{1}{\left(\frac{P_1}{P_2}\right)^{\frac{k-1}{k}}}\right)\eta / n \tag{16}$$

Where T_m is the expander output torque; is the expander output power; C_p is the specific heat capacity at a constant pressure; T_{on} is the expander outlet temperature; T_{in} is the expander inlet temperature, k is the isentropic index, P_1 is the expander inlet pressure, and P_2 is the expander outlet pressure, η the expander efficiency, and n is the expander/generator speed.

3.3. Mathematical Model of PMSG

Prior to mathematical modeling of PMSG, the following assumptions are made in this paper:

(1) PMSG stator winding Y-connected, symmetrical distribution of three-phase windings;

(2) Ignore the stator winding leakage inductance, not counting the motor hysteresis loss;

(3) Ignore core saturation;

(4) There is no damping winding on the rotor.

According to the above assumptions, the mathematical model of the PMSG in the two-phase stationary coordinate system (αβ coordinate system) is as follows [15]:

Stator voltage equation:

$$\begin{bmatrix} u_\alpha \\ u_\beta \end{bmatrix} = \begin{bmatrix} R_s + \frac{d}{dt}L_d & \omega_r(L_d - L_q) \\ -\omega_r(L_d - L_q) & R_s + \frac{d}{dt}L_q \end{bmatrix}\begin{bmatrix} i_\alpha \\ i_\beta \end{bmatrix} + \left[(L_d - L_q)(\omega_s i_d - i_q)\right]\begin{bmatrix} \cos\theta_r \\ \sin\theta_r \end{bmatrix} \tag{17}$$

In the formula, i_α , i_β are the stator current $\alpha\beta$-axis component; u_α , u_β are the stator winding phase voltage $\alpha\beta$-axis component; R_s are the stator winding resistance; ψ_α ,ψ_β are the stator winding flux linkage $\alpha\beta$-axis. L_d , L_q are the stator dq-axis inductance; and ω_r , θ_r are the rotor rotation electric angle and rotor pole angle, respectively.

Stator flux equation:

$$\begin{bmatrix} \Psi_\alpha \\ \Psi_\beta \end{bmatrix} = L_q\begin{bmatrix} i_\alpha \\ i_\beta \end{bmatrix} + \left[(L_d - L_q)i_d\right]\begin{bmatrix} \cos\theta_r \\ \sin\theta_r \end{bmatrix} \tag{18}$$

Taking the stator flux linkage as the state variable, and L_d=L_q, the generator state equation is obtained as:

$$\frac{d}{dt}\begin{bmatrix} \Psi_\alpha \\ \Psi_\beta \end{bmatrix} = \begin{bmatrix} \frac{R_s}{L_d} & 0 \\ 0 & \frac{R_s}{L_d} \end{bmatrix}\begin{bmatrix} \Psi_\alpha \\ \Psi_\beta \end{bmatrix} + \begin{bmatrix} u_\alpha \\ u_\beta \end{bmatrix} \tag{19}$$

In this coordinate system ψ_α and ψ_β can be derived using the inverse electric potential integral:

$$\Psi_\alpha = \int(u_\alpha + R_s i_\alpha)dt \tag{20}$$

$$\Psi_\beta = \int(u_\beta + R_s i_\beta)dt \tag{21}$$

Mathematical model of electromagnetic torque:

$$T_e = \frac{3}{2}n_p(\Psi_\alpha i_\beta - \Psi_\beta i_\alpha) \tag{22}$$

Where n_p is the number of generator pole pairs.

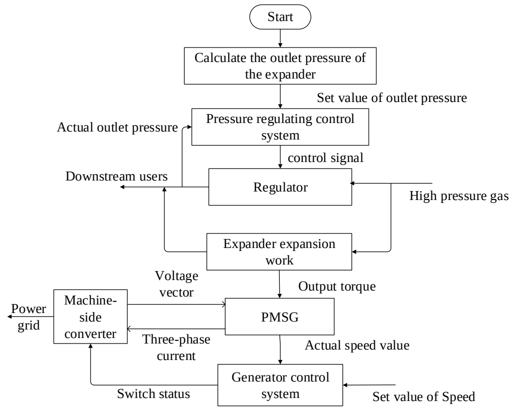

Fig.2 Control system flow chart

4. RESEARCH OF CONTROL STRATEGY

4.1. Control plan

In this paper, the regulator system and the power generation system are controlled separately. The overall system flow chart is shown in Figure 2. The pressure regulation system adopts fuzzy PI control to keep the outlet pressure stable when the gas consumption of downstream users changes, resulting in changes in the outlet pressure of the expander. The expander expands according to the pressure difference between the high-pressure gas at the inlet and the low-pressure gas at the outlet after it has been stabilized by the pressure regulating system, and outputs torque to the PMSG; The power generation system adopts a direct torque control method combining fuzzy PI and model prediction. When the expander's output torque changes due to changes in the gas consumption of downstream users, the control generator quickly follows the expander's output torque and keeps the torque and flux linkage stable to improve the quality of power generation.

4.1.1. Fuzzy PI based control of pressure regulation system

In this paper, the fuzzy PI control strategy is used to control the regulator system, and the structure diagram of this control system is shown in Figure 3. The system inputs the error of the expander outlet pressure into the fuzzy PI controller of the regulator system, and the controller adjusts the PI parameters in real time according to the error of the outlet pressure and the rate of change of the error, and outputs the valve opening control signal to the regulator, thus controlling the expander outlet pressure, and then controlling the output torque of the expander.

4.1.2. Fuzzy PI-based PMSG direct torque control

The outer loop of this DTC algorithm is the speed loop,

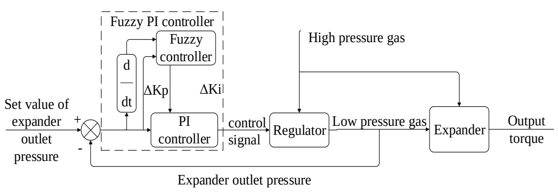

Fig.3 Structure diagram of control strategy of pressure regulating system

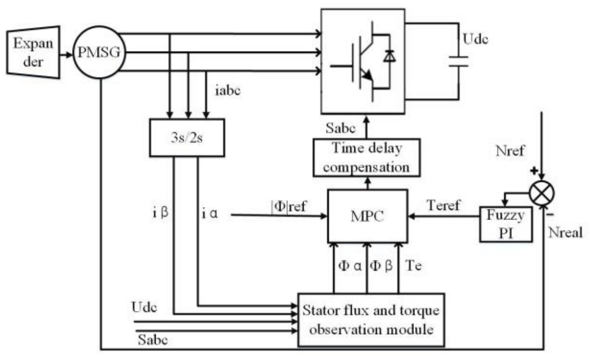

Fig.4 Structure diagram of generator control strategy

which is controlled by a fuzzy PI controller. The composition of the control system is shown in Figure 4. The speed error of the PMSG is input to the fuzzy PI controller of the power generation system, and the PI parameters are adjusted in real time according to the PMSG speed error and the error change rate, and the torque control signal is output as the torque given value of the inner-loop MPC controller. At the same time, based on the error between the given and actual values of flux linkage and torque, each voltage vector in the prediction time domain is calculated, and the voltage vector that minimizes the optimized objective function is selected as the output of the model prediction controller, thereby controlling the generator and thus suppressing the generator torque fluctuations.

The purpose of model predictive control is to keep the torque as well as the flux linkage stable when the expander outlet pressure fluctuates, so the squared difference between the torque and flux linkage and their set values is chosen as the optimization objective function in this paper:

$$J = (T_{\mathrm{e}}^{*} - T_{e})^{2} + (\Psi^{*} - \Psi)^{2} \tag{23}$$

4.2. Fuzzy PI Rules

The fuzzy PI controller's consists of a fuzzy controller and a PI controller. The controller adjusts the PI parameters in real time according to the input error and its rate of change, as well as the established fuzzy rules, and then realizes the self-tuning of PI parameters and outputs the corresponding control signal [16], so as to reduce the impact of working condition changes on the system.

In this paper, two dual-input single-output fuzzy PI controllers are used to control a gas regulator system and a power generation system, respectively. The fuzzy controller in the fuzzy PI controller inputs the proportional coefficient variable ΔKp and the integral coefficient ΔKi into the PI controller according to the corresponding fuzzy rules to

Tab.2 ΔKp rule

ec	**e**						
	NB	**NM**	**NS**	**ZO**	**PS**	**PM**	**PB**
NB	PB	PM	PS	PB	NM	NS	ZO
NM	PB	PM	PS	PM	NS	ZO	PS
NS	PM	PS	PS	PS	PS	PS	PS
ZO	PM	PS	PS	ZO	PS	PS	PM
PS	PS	PS	PS	PS	PS	PS	PM
PM	PS	ZO	NS	PM	PS	PM	PB
PB	ZO	NS	NM	PB	PS	PM	PB

Tab.3 ΔKi rules

ec	e						
	NB	NM	NS	ZO	PS	PM	PB
NB	PB	PB	PB	PB	NB	NM	NB
NM	PB	PB	PB	PM	NM	NS	NM
NS	PM	PM	PM	PS	PS	ZO	NB
ZO	PM	PS	PM	PS	PM	PS	PM
PS	NS	ZO	PS	PS	PM	PM	PM
PM	NM	NS	NS	PM	PB	PB	PB
PB	NB	NM	NB	PB	PB	PB	PB

realize the PI parameter adaptation adjustment. The inputs of the two fuzzy PI controllers are the error e and error rate of change ec of the expander outlet pressure and generator speed, and the outputs are the regulator valve opening control signal and generator torque control signal, respectively. Based on experience, this paper divides the fuzzy sets into seven theoretical domains, which are {"Negative Big", "Negative Medium", "Negative Small", "Zero", "Positive small", "Positive medium", "Positive Big"}, namely {"NB", "NM", "NS", "ZO", "PS", "PM", "PB"}.In order to implement fuzzy PI control, it is necessary to understand the influence of PI parameters on the system. In PI control, increasing the proportionality coefficient can shorten the system response time and reduce the stability error, but too large a proportionality coefficient can lead to increased system overshoot and system oscillation time. Increasing the integration coefficient can eliminate the system steady-state error, and as the integration coefficient increases, it will reduce the time required to eliminate the steady-state error, but too large an integration coefficient will cause overshoot, and too small will affect the control accuracy.

According to the experience, the fuzzy PI Degree of Membership Function uses the trigonometric function, as shown in Figure 5. The corresponding fuzzy rules are obtained based on the experiments, and the control rules of Δ Kp and Δ Ki for the fuzzy PI controller are given in Table 2 and Table 3.

4.3. Model prediction direct torque control

Model Predictive Direct Torque Control (MPDTC) predicts the torque and flux linkage under the action of each alternate voltage vector at the next moment by establishing the prediction models of torque and flux linkage, and then selects the optimal voltage vector based on the constructed optimal objective function and compensates the system with delay to achieve the purpose of reducing the fluctuation of generator torque.

4.3.1. Prediction model

In this paper, we discretize (19) according to the forward Eulerian discretization method to obtain the flux linkage prediction model of PMSG:

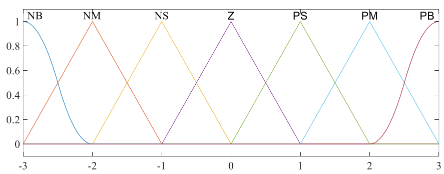

Fig.5 Degree of Membership Function

$$\frac{d}{dt}\begin{bmatrix}\Psi_\alpha(k)\\ \Psi_\beta(k)\end{bmatrix} = T_s\begin{bmatrix}\frac{R_s}{L_d} & 0\\ 0 & \frac{R_s}{L_d}\end{bmatrix}\begin{bmatrix}\Psi_\alpha(k)\\ \Psi_\beta(k)\end{bmatrix} + T_s\begin{bmatrix}u_\alpha(k)\\ u_\beta(k)\end{bmatrix} \tag{24}$$

$$\begin{bmatrix}\Psi_\alpha(k+1)\\ \Psi_\beta(k+1)\end{bmatrix} = \begin{bmatrix}\Psi_\alpha(k)\\ \Psi_\beta(k)\end{bmatrix} + \frac{d}{dt}\begin{bmatrix}\Psi_\alpha(k)\\ \Psi_\beta(k)\end{bmatrix} \tag{25}$$

Where Ts is the sampling time.

Similarly, the current prediction model of the motor can be obtained:

$$\begin{bmatrix}i_\alpha(k+1)\\ i_\beta(k+1)\end{bmatrix} = \begin{bmatrix}\frac{1}{L_d} & 0\\ 0 & \frac{1}{L_d}\end{bmatrix}\begin{bmatrix}\Psi_\alpha(k+1)\\ \Psi_\beta(k+1)\end{bmatrix} \tag{26}$$

Then the torque prediction model of the motor can be obtained according to (22):

$$\begin{aligned}T_e(k+1) = &\frac{3}{2}n_p(\Psi_\alpha(k+1)i_\beta(k+1)\\ &-\Psi_\beta(k+1)i_\alpha(k+1))\end{aligned} \tag{27}$$

4.3.2. Time delay compensation

In MPC, each control cycle needs to be optimized and calculated. Therefore, when the optimal voltage vector is calculated and output, the relevant variables of the system will change, resulting in the output voltage vector is no longer the optimal voltage vector at the current moment, therefore, delay compensation is required.

In this paper, we eliminate the control delay by predicting the trajectories of the state variables over the next N (N ≥ 1) cycles of the system. The larger the chosen N, the higher the control accuracy, but the larger the computational effort. In order to reduce the system computation and improve the real-time performance, and at the same time to ensure the system control accuracy, this paper selects different prediction periods for predictive control through simulation tests, and the system control effect is relatively good and the computation is minimal when N=2. Its prediction model expression is:

$$\begin{bmatrix}\Psi_\alpha(k+2)\\ \Psi_\beta(k+2)\end{bmatrix} = \begin{bmatrix}\Psi_\alpha(k+1)\\ \Psi_\beta(k+1)\end{bmatrix} + \frac{d}{dt}\begin{bmatrix}\Psi_\alpha(k+1)\\ \Psi_\beta(k+1)\end{bmatrix} \tag{28}$$

$$\begin{bmatrix}i_\alpha(k+2)\\ i_\beta(k+2)\end{bmatrix} = \begin{bmatrix}\frac{1}{L_d} & 0\\ 0 & \frac{1}{L_d}\end{bmatrix}\begin{bmatrix}\Psi_\alpha(k+2)\\ \Psi_\beta(k+2)\end{bmatrix} \tag{29}$$

$$\begin{aligned}T_e(k+2) = &\frac{3}{2}n_p(\Psi_\alpha(k+2)i_\beta(k+2)\\ &-\Psi_\beta(k+2)i_\alpha(k+2))\end{aligned} \tag{30}$$

4.3.3. Model prediction direct torque control process

In summary, the MPDTC algorithm flow is as follows:

(1) The αβ-axis components $\psi_\alpha(k)$,ψ_β(k) of the flux linkage of the generator at moment k, the converter output DC voltage U_{dc}, the torque given by the output of the outer loop fuzzy PI controller $Te*$, and the flux linkage value $\psi*$, are read and the torque $Te(k)$ is obtained according to equation (28);

Tab.4 Simulation parameters of PMSG

Parameters	Value	Parameters	Value
Stator resistance R_s/Ω	1.3	sampling time /s	1e-6
L_q /mH	0.75	Load ResistanceR/Ω	50
Permanent magnet flux /Wb	0.4	Load capacitanceC/μF	200
Number of pole pairsp	2	Stator flux /Wb	0.4

(2) Bringing the above state variables into the prediction model, the values of the flux linkage $\psi\alpha(k+1)$,$\psi\beta(k+1)$ and the torque $Te(k+1)$ at the moment k+1 are calculated;

(3) The torque and flux linkage at the moment k+1 are delayed and compensated, and all voltage vectors acting on $\psi\alpha(k+2)$,$\psi\beta(k+2)$ and torque $Te(k+2)$ with their set values ψ^*, Te^* are brought into the optimization objective function, and the voltage vector that minimizes the optimization objective function is selected.

(4) The resulting voltage vector is output to the generator for control.

5. Simulation Experiment

To verify the effectiveness of the above methods, this paper develops a system based on Matlab with the conventional PI-based direct torque algorithm, and the direct torque control algorithm based on fuzzy PI and model predict control. The simulation parameters of the PMSG are shown in Table 4.

In the simulation experiment, the expander is given an outlet pressure of 485 KPa, which jumps to 590 KPa at 0.05s. The output torque of the expander is used as the input torque of the PMSG.

Figure 6 shows the waveform of expander outlet pressure and output torque. From the figure, it can be seen that both control algorithms can keep the expander outlet pressure and output torque stable when the given value of expander outlet pressure changes abruptly, but the expander pressure regulation system with fuzzy PI control algorithm has faster response time. In Fig. a), when the expander outlet pressure changes abruptly, the output torque of the expander has a large downward impulse according to equation (17) because the abrupt change is large and the abrupt change time is short.

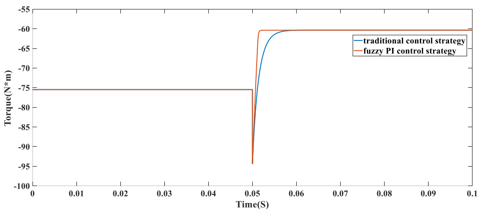

a) Expander outlet pressure waveform of different control strategy

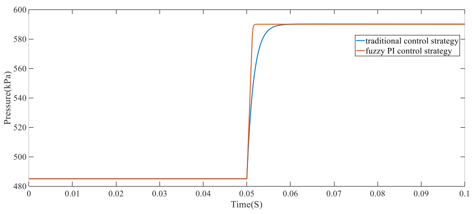

b) Expander Output torque waveform of different control strategy

Fig.6 Waveform diagram of expander outlet pressure and output torque

Figure 7 shows the waveforms of torque and speed under different control methods of PMSG. From Fig. (a) and (b), it can be seen that, under the DTC algorithm, the variation range of torque is ±1.5N*m and the fluctuation range of speed is ±0.09r/min at a given speed of 1000r/min; at a given speed of 800r/min, the variation range of torque is ±1.20N*m and the fluctuation range of speed is ±0.1r/min. In Figs. c) and d), with the fuzzy PI and MPDTC algorithms, the variation range of torque is ±0.24N*m and the fluctuation range of speed is ±0.03r/min at the given speed of 1000r/min; at the given speed of 800r/min, the fluctuation range of torque is ±0.24N*m and the fluctuation range of speed is ±0.03r/min.

Figure 8 shows the three-phase current waveforms of generator output under conventional DTC algorithm and fuzzy PI MPDTC. It can be seen from the figure that the fuzzy PI model predictive control algorithm reduces the fluctuation range of the generator output three-phase

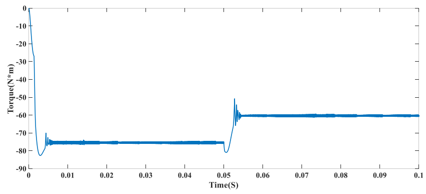

a) DTC algorithm torque waveform

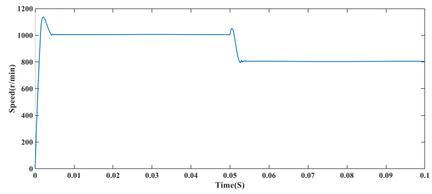

b) DTC algorithm speed waveform

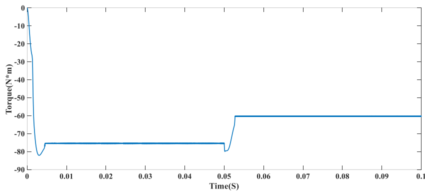

c) Fuzzy PI model predicts DTC algorithm torque waveform

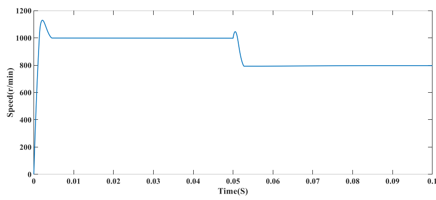

d) Fuzzy PI model predicts the waveform of DTC rotation speed

Fig.7 Comparison of simulation waveform diagrams of different generator control algorithms current by 65.6%, respectively, compared to the

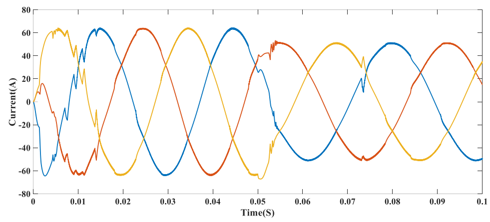

a) Direct torque control three-phase current waveform

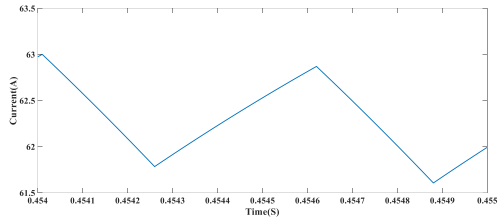

b) Direct torque control three-phase current local waveform

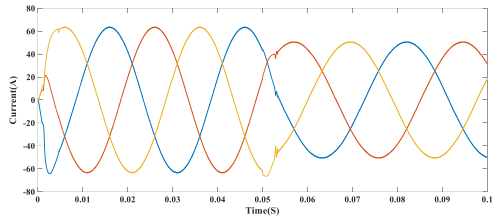

b) Fuzzy PI model predicts three-phase current waveform

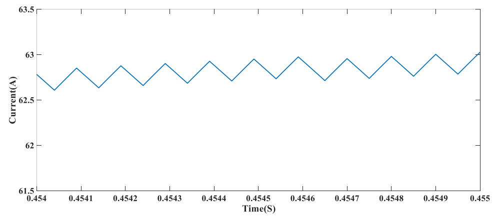

d) Fuzzy PI model predicts the local waveform of three-phase current

Fig.8 Motor three-phase current waveform diagram

conventional direct torque control.

Acknowledgements

This work was supported by the High Level Innovation Team Construction Project of Beijing Municipal Universities (No. IDHT20190506), the Key Science and Technology Plan Project of Beijing Municipal Education Commission of China (No. KZ201810016019) and the BUCEA Post Graduate Innovation Project.

REFERENCES:

[1] Y Xiong, S An, P Xu, Y Ding, C Li, Q Zhang, H Chen. A novel expander-de/pending natural gas pressure regulation configuration: Performance analysis[J]. Applied Energy, 2018, 220:21-35.

[2] Xie Wenjin. Research on gas electric pressure regulation and remote measurement and control system [D]. Chongqing University, 2016.(in Chinese)

[3] X Hao, AN Xaioran, WU Bo, HE Shaoping. Application of a support vector machine algorithm to the safety precaution technique of medium-low pressure gas regulators[J]. Journal of Thermal Science, 2018, 27(01):74-77.

[4] Ouhrouche M , Errouissi R , Trzynadlowski A M , et al. A Novel Predictive Direct Torque Controller for Induction Motor Drives[J]. IEEE Transactions on Industrial Electronics, 2016, 63(8):5221-5230.

[5] Zhu Renshuai. Simulation and experimental research of permanent magnet synchronous motor control system [D]. Shenyang University of Technology, 2019. (in Chinese)

[6] Chen Guangwei. Research on Direct Torque Control of Permanent Magnet Direct Drive Wind Power Generation System Machine-side Converter [D]. Hunan University, 2015. (in Chinese)

[7] Y Wang, L Geng, WJ Hao, W Xiao. Control Method for Optimal Dynamic Performance of DTC based PMSM drives[J]. IEEE Transactions on Energy Conversion, 2018:1-1.

[8] A Ghamri, R Boumaaraf, MT Benchouia, H Mesloub, A Goléa, N Goléa. Comparative study of ANN DTC and conventional DTC controlled PMSM motor[J]. Mathematics and Computers in Simulation (MATCOM), 2020, 167.

[9] Thamizhazhagan P , Sutha S . Adaptive vector control reference strategy based speed and torque control of Permanent Magnet Synchronous Motor[J]. Microprocessors and Microsystems, 2020, 74:103007.

[10] Liu Yidi. Theoretical analysis of output torque of single screw expander and research exploration of performance evaluation index[D]. Beijing University of Technology, 2015. (in Chinese)

[11] Zhang Xiaofan. Research on neural network adaptive control method of gas electric pressure regulating system[D]. Chongqing University, 2018. (in Chinese)

[12] Bodson, M., Chiasson, N J., Novotnak, T R., Rekowski, B R.. High-performance nonlinear feedback control of a permanent magnet stepper motor[J]. Control Systems Technology, IEEE Transactions on, 1993.

[13] Bechlioulis C P , Rovithakis G A . Robust Adaptive Control of Feedback Linearizable MIMO Nonlinear Systems With Prescribed Performance[J]. IEEE Transactions on Automatic Control, 2008, 53(9):2090-2099.

[14] Li Xueping. Research on control strategy of permanent magnet direct drive waste heat power generation system[D]. Hunan University, 2018. (in Chinese)

[15] Jiang Xuexiang. Research on direct torque control of permanent magnet direct drive wind power converter system [D]. Hunan University of Technology, 2015. (in Chinese)

[16] Kluska J , Zabinski T . PID-Like Adaptive Fuzzy Controller Design Based on Absolute Stability Criterion[J]. IEEE Transactions on Fuzzy Systems, 2019:1-1